Microbiology (2005), **151**, 1229–1238 DOI 10.1099/mic.0.27375-0

Genome-based *in silico* detection of putative manganese transport systems in *Lactobacillus plantarum* and their genetic analysis

Masja N. Nierop Groot,[1] Eline Klaassens,[1] Willem M. de Vos,[1] Jean Delcour,[2] Pascal Hols[2] and Michiel Kleerebezem[1]

Correspondence
Michiel Kleerebezem
Michiel.Kleerebezem@nizo.nl

[1]Wageningen Centre for Food Sciences, NIZO Food Research, Kernhemseweg 2, PO Box 20, 6710 BA Ede, The Netherlands

[2]Unité de Génétique, Institut des Sciences de la Vie, Université catholique de Louvain, 5 Place Croix du Sud, Louvain-la-Neuve, 1348, Belgium

Manganese serves an important function in *Lactobacillus plantarum* in protection against oxidative stress and this bacterium can accumulate Mn^{2+} up to millimolar levels intracellularly. Although the physiological role of Mn^{2+} and the uptake of this metal ion have been well documented, the only uptake system described so far for this bacterium is the Mn^{2+}- and Cd^{2+}-specific P-type ATPase (MntA). Recently, the genome of *L. plantarum* WCFS1 has been sequenced allowing *in silico* detection of genes potentially encoding Mn^{2+} transport systems, using established microbial Mn^{2+} transporters as the query sequence. This genome analysis revealed that *L. plantarum* WCFS1 encodes, besides the previously described *mntA* gene, an ABC transport system (*mtsCBA*) and three genes encoding Nramp transporters (*mntH1*, *mntH2* and *mntH3*). The expression of three (*mtsCBA*, *mntH1* and *mntH2*) of the five transport systems was specifically derepressed or induced upon Mn^{2+} limitation, supporting their role in Mn^{2+} homeostasis in *L. plantarum*. However, in contrast to previous reports, *mntA* expression remains below detection levels in both Northern and real-time RT-PCR analysis in both Mn^{2+} excess and starvation conditions. Growth of WCFS1 derivatives mutated in *mntA*, *mtsA* or *mntH2*, or both *mtsA* and *mntH2* appears unaffected under Mn^{2+} excess or Mn^{2+} limitation. Moreover, intracellular Mn^{2+} concentrations remained unaltered in these mutants compared to the wild-type. This may suggest that this species is highly adaptive in response to inactivation of these genes or, alternatively, that other transporters that have not yet been identified as Mn^{2+} transporters in bacteria are involved in Mn^{2+} homeostasis in *L. plantarum*.

Received 3 June 2004
Revised 16 November 2004
Accepted 14 January 2005

INTRODUCTION

Bacteria depend on efficient uptake systems to import essential trace metals from the environment. The Mn^{2+} ion is an important trace metal that is required for growth and survival of most bacteria. However, several lactic acid bacteria (LAB), including *Lactobacillus plantarum*, are known to have higher requirements for Mn^{2+} and accumulate high intracellular levels of Mn^{2+} (Archibald & Fridovich, 1981a, b; Nierop Groot & de Bont, 1999). The physiological role of Mn^{2+}, and the uptake of this metal ion, have been well documented for *L. plantarum* (Archibald & Fridovich, 1981b; Archibald & Duong, 1984). The intracellular pool of Mn^{2+} in this species is used to scavenge toxic oxygen species, especially O_2^-, and enables this bacterium to survive oxidative stress conditions. The millimolar level of intracellular Mn^{2+} thereby compensates for the lack of superoxide dismutase (SOD), which is present in most oxygen-tolerant micro-organisms.

While evidence for the presence of an active Mn^{2+} uptake system in *L. plantarum* has been available for a long time (Archibald & Duong, 1984), the only uptake system described for this species to date is a Mn^{2+}- and Cd^{2+}-specific P-type ATPase (MntA) (Hao *et al.*, 1999a). Functionality of MntA from *L. plantarum* has been demonstrated in *Escherichia coli* where its expression conferred increased sensitivity and uptake of Cd^{2+}, which is a known alternative substrate for Mn^{2+} (Hao *et al.*, 1999a). An *mntA*-mutant derivative of strain ATCC 14917 was unable to grow in medium containing less than 20 mM Mn^{2+}.

Two additional families of Mn^{2+} transport systems have been identified in several other bacterial species. One of these Mn^{2+} transporters belongs to the ATP-binding cassette (ABC) family of transporters and was first described for *Synechocystis* sp. PCC6803 (Bartsevich & Pakrasi, 1995) and later also identified in several Gram-positive bacteria (reviewed by Claverys, 2001). These transporters are

encoded by an operon and contain a solute-binding extracytoplasmic protein, a cytoplasmic ATP-binding protein and an integral membrane protein. In Gram-positive bacteria, the cell-surface substrate-binding components of these Mn^{2+} transporters belong to the lipoprotein receptor antigen I (LraI) family and were initially identified as adhesins that play a role in virulence (Sampson *et al.*, 1994). However, subsequent research established their role as extracytoplasmic substrate recognition subunit of Mn^{2+}-specific ABC transporters in *Streptococcus pneumoniae* (PsaA) and *Streptococcus gordonii* (ScaA) (Dintilhac *et al.*, 1997; Kolenbrander *et al.*, 1998). *S. gordonii sca* mutants displayed decreased Mn^{2+} uptake and impaired growth in media containing less than 0·5 μM Mn^{2+}, and mutant cells were hypersensitive to oxygen in Mn^{2+}-deficient medium (Jakubovics *et al.*, 2002). By analogy, a requirement for increased Mn^{2+} concentrations in the growth medium has been reported for an *S. pneumoniae psaA* mutant (Dintilhac *et al.*, 1997) and a *Streptococcus pyogenes mtsA* mutant (Janulczyk *et al.*, 2003). PsaA/ScaA homologues have been identified in at least nine additional species of *Streptococcus* and also in bacteria belonging to other genera (for a review see Claverys, 2001). Mn^{2+} uptake by ABC transporters has been experimentally demonstrated in *Salmonella enterica* serovar Typhimurium (Kehres *et al.*, 2002; Kehres & Maguire, 2003) and specificity for both iron and manganese was shown for *Yersinia pestis* (Bearden & Perry, 1999), *S. pyogenes* (Janulczyk *et al.*, 2003) and *Streptococcus mutans* (Paik *et al.*, 2003).

A third type of transporter has been reported to be involved in Mn^{2+} uptake in bacteria. These bacterial transporters are homologues of the mammalian Nramp (natural resistance-associated macrophage protein) transporters for divalent metal ions, which act as regulators of host susceptibility to intracellular infections (reviewed by Forbes & Gros, 2001). Similar systems have been identified in *Bacillus subtilis* (Que & Helmann, 2000), *Salmonella typhimurium* (Kehres *et al.*, 2000) and *E. coli* (Makui *et al.*, 2000), and confer high-affinity uptake of Mn^{2+}. Molecular studies of the enterobacterial (Kehres *et al.*, 2000) and *B. subtilis* (Que & Helmann, 2000) *nramp* genes demonstrated that they encode proton-stimulated, highly selective Mn^{2+} transporters that play a role in the bacterial response to oxidative stress (Kehres *et al.*, 2000).

Since Mn^{2+} serves an important function in oxygen tolerance of *L. plantarum*, one or more highly efficient systems to import this metal ion are expected to be encoded by this organism. Of the three known classes of bacterial Mn^{2+} transporters, to date only the P-type ATPase has been described for *L. plantarum*, while Nramp and ABC-transporters have been described in species that have low Mn^{2+} requirements and that have superoxide dismutase activity. In this paper we use protein sequences of established bacterial Mn^{2+} transport systems to identify candidate Mn^{2+} transport system encoding genes in the *L. plantarum* WCFS1 genome. In addition, we establish their induced expression by *L. plantarum* in response to Mn^{2+} limitation and, by mutation analysis, study their contribution to the extraordinary high Mn^{2+} levels accumulated by this bacterium.

METHODS

Bacterial strains and culturing conditions. Strains, plasmids and oligonucleotides used in this study are listed in Tables 1 and 2. *L. plantarum* was grown statically, unless indicated otherwise, in either MRS broth (Merck) or a chemically defined medium (CDM; Kets *et al.*, 1994). *E. coli* strains were grown with aeration at 37 °C in Tryptone Yeast (TY) medium (Sambrook *et al.*, 1989). Antibiotics were added to the medium where appropriate at the following

Table 1. Bacterial strains and plasmids used in this study

Strain/plasmid	Relevant characteristics	Reference
Strains		
E. coli DH5α		Hanahan (1983)
L. plantarum WCFS1	Sequenced strain	Kleerebezem *et al.* (2003)
NZ7257	WCFS1 derivative, Δ*mtsA*	This study
NZ7259	WCFS1 derivative, Δ*mntH2*	This study
NZ7260	WCFS1 derivative, Δ*mtsA*Δ*mntH2*	This study
NZ7256	WCFS1, *mntA* disruption mutant	This study
Plasmids		
pGEM-T	PCR cloning vector; Ap^R	Promega
pCRblunt	Cloning vector for blunt PCR fragments; Km^R	Promega
pNZ7260	pGEM-T containing a 620 bp PCR fragment of *mtsA L. plantarum*	This study
pUC18ery	Ap^R Em^R	Van Kranenburg *et al.* (1997)
pNZ7256	pUC18ery derivative for disruption of *mntA*	This study
pNZ7257	pUC18ery derivative; Ap^R Em^R; knock-out construct *mtsA*	This study
pNZ7258	pUC18ery derivative; Ap^R Em^R; harbouring a 649 bp fragment of *mntH2*	This study
pNZ7259	pNZ7258 derivative; Ap^R Em^R; knock-out construct *mntH2*	This study

Table 2. Oligonucleotides used in this study

Restriction sites introduced in the oligonucleotide sequence are underlined.

Oligonucleotide	Sequence (5′–3′)
LPATP3	GCCTGAATTCTGCAGGCACAATGGTGGTA-GC
LPATPR3	CGGAGGATCC CTTCGTTTGGCTAAATCA-GTGG
LPATPF3	TGGGCCTATAATTCGGTTGTG
LPATPR3	CGAGCCATCACCAACAATTAC
LPATPF4	ATGACGACGACGGTCGTGTTAG
LPATPR4	CCGCAAAAACATCGTGGTCAAAG
LPATPF6	TCAGCCATGGAAACGAAATTAATTGCAC
LPATPR6	ACTGTCTAGACAACCGAATTATAGGCC
LPMNTH1F	GCATTACTTTCTGTGATCC TG
LPMNTH1R	CATTGTACAAGTCAACGAACC
LPMNTH2AF	CATGCTAATGTCTGTCATCTTG
LPMNTH2AR	CATAAAGACCGAAGAATGAAGG
LPMNTH2BF	AATATCTAGACAGCAACTTGCTGCAGC
LPMNTH2BR	AAAAGTCGACGCTGTCAACATAAATAGCG
LPMNTH3F	GACCGTCGGCATTATTTTTGG
LPMNTH3R	GTCAAAGTAGCTATGTGAATGG
16SP1	GCGGCGTGCCTAATACATGC
16SP2	ATCTACGCATTTCACCGCTAC
LPABCSEQ	CTGTATGCCACGGTGAGG
LPH1SEQ	TCTTAGCGTGATCC TTCG
LPH2SEQ	GGAACCTCGATGGTACCG
QMNTAF3	CGAAGCGCTAGTTGGTGAAG
QMNTAR3	CTAAAGCCGGTTGCTGTGTG
QMNTH2F	CGCCACTTTCTGGTGCTTTA
QMNTH2R	CAATCTTCCGCGTTTGTGAG
Q16Sforw	TGATCC TGGCTCAGGACGAA
Q16Srev	TGCAAGCACCAATCAATACCA
QMTSAF	AACCACGGCCCACTGATATT
QMTSAR	GCCATTACCGCCAGTTTCA
QMNTH1F	GCCGTGATTCTCTTCGTCTTC
QMNTH1R	GACAATCC GACTAGTTGGGACA

concentrations: erythromycin (Em) 10 μg ml^{-1} (*L. plantarum*) and 250 μg ml^{-1} (*E. coli*); ampicillin (Ap) 100 μg ml^{-1} (*E. coli*); kanamycin (Km) 50 μg ml^{-1} (*E. coli*).

DNA isolation, manipulations and sequence analysis. JetStar columns (Genomed GmbH) were used for large-scale isolations of *E. coli* plasmid DNA following the instructions of the manufacturer. Small-scale plasmid DNA isolations and standard recombinant DNA techniques were performed as described by Sambrook *et al.* (1989). *L. plantarum* was transformed by electroporation (Aukrust & Blom, 1992) and *E. coli* cells were transformed by the $CaCl_2$ procedure (Sambrook *et al.*, 1989). PCR amplifications were carried out with an automated thermal cycler (Perkin-Elmer) using either *Taq* DNA polymerase (Gibco-BRL Life Technologies) or *Pwo* polymerase (Roche Diagnostics). DNA was isolated from agarose gels by using a QIAEX II gel extraction kit (Pharmacia Biotech). A non-radioactive dioxygenin (DIG) DNA labelling and detection kit (Roche Diagnostics) was used to label and detect probes for Southern blotting, according to the manufacturer's instructions.

Construction of *mntA*, *mtsA* and *mntH2* mutants. To inactivate the *mtsA* and *mntH2* genes in *L. plantarum* WCFS1 by double cross-over recombination, we used the non-replicating vector pUC18ery (Van Kranenburg *et al.*, 1997). For the introduction of a deletion in *mtsA*, two fragments flanking the region to be deleted were amplified by PCR. Using primers LPATPF3 and LPATPR3, a 860 bp fragment was obtained corresponding to the sequence downstream of the 3′ end of the coding region of *mtsA* (fragment B). Primers LPATPF4 and LPATPR4 generated an 822 bp PCR fragment that contains 355 bp of the 5′ end of *mtsA* and 467 bp of the 3′ end of *mtsB* (fragment A). Both PCR products were cloned in pGEM-T (Promega) and the resulting plasmids were used for sequence verification of the fragments. Subsequently, the *mtsA*-flanking fragments were reisolated as a *Nco*I–*Sac*I (fragment A) or *Nco*I–*Sal*I fragments (fragment B) and cloned in *Sal*I/*Sac*I-digested pUC18ery, resulting in pNZ7257. This construct was introduced into *L. plantarum* by electroporation and primary integrants were selected on plates containing Em. Integration of pNZ7257 at the *mts* locus was confirmed by Southern blotting and one of the integrants was cultured without selection pressure to allow the second cross-over event, resulting in an Em^S phenotype. After 100 generations, three candidate mutants (Em^S) were obtained and Southern analysis confirmed that two strains contained the 575 bp deletion in *mtsA* (data not shown).

The *mntH2* gene was inactivated by a 617 bp deletion at the 3′ end of the gene using the double cross-over recombination strategy described above. A 649 bp fragment, located at the 5′ end of *mntH2*, was amplified using primers LPMNTH2AF and LPMNTH2AR and cloned into pCRblunt (Promega), reisolated from the resulting plasmid as a *Sac*I–*Xba*I fragment and subcloned into *Sac*I/*Xba*I-digested pUC18ery, yielding pNZ7258. A 714 bp fragment located downstream of the stop codon of *mntH2* was amplified using primers LPMNTH2BF and LPMNTH2BR. The PCR product obtained was digested with *Sal*I and *Xba*I and cloned in similarly digested pNZ7258, yielding the *mntH2* knock-out plasmid pNZ7259. This plasmid was used to obtain the *mntH2* mutant derivatives of both wild-type *L. plantarum* WCFS1 and its *mtsA* deletion derivative. Mutant strains were designated NZ7257, NZ7259 and NZ7260 for the *mtsA*, *mntH2* and the *mtsA-mntH2* mutants, respectively.

The *mntA* gene in *L. plantarum* WCFS1 was disrupted by single cross-over plasmid integration. To create the integration plasmid pNZ7256, an 1143 bp internal fragment of *mntA* was amplified by PCR using the primers LPATP3 and LPATPR3, and cloned into pUC18ery using the *Eco*RI and *Bam*HI restriction sites introduced in the primer sequences. Plasmid pNZ7256 was transformed into *L. plantarum* by electroporation and candidate integrants were selected on MRS agar plates containing 10 μg Em ml^{-1}. Correct integration of pNZ7256 in the *mntA* locus was confirmed by PCR and Southern blotting, and a single *mntA* disruption mutant (NZ7256) was used in subsequent studies.

Intracellular manganese analysis. The amount of Mn^{2+} accumulated in the wild-type and its mutant derivatives was determined. Overnight-grown cells in CDM (300 μM or 1·5 μM Mn^{2+}) were diluted 1 : 100 in CDM (300 μM or 1·5 μM Mn^{2+}) and cultured overnight. Cells were harvested by centrifugation and washed three times with CDM without manganese. The resulting pellet was suspended in Millipore water and cells were mechanically disrupted in the presence of zirconium beads in a FastPrep FP120 (Savant Instruments). Cell debris was removed by centrifugation and the remaining supernatant was diluted in MilliQ for determination of Mn and protein (Bradford, 1976) concentration. Mn^{2+} concentrations were determined by Inductivity-Coupled Plasma Atomic Emission Spectrometry (ICP-AES).

RNA isolation, Northern blotting and primer extension. Overnight-grown cells of *L. plantarum* in CDM (containing 300 μM

$MnSO_4$) were washed in CDM without Mn^{2+} and diluted 1 : 100 in CDM with variable $MnSO_4$ concentrations (1·5–300 μM), and incubated overnight at 37 °C. One millilitre of each of these cultures was used to inoculate 50 ml CDM with the same $MnSO_4$ concentration as used for the overnight culture. Cells were harvested at an OD_{600} of 0·4–0·5 and RNA was isolated by the Macaloid method described by Kuipers *et al.* (1993) with the adaptation that prior to disruption cells were incubated with lysozyme for 5 min on ice. RNA was separated on 1 % formaldehyde-MOPS agarose gels, blotted and hybridized as was described previously (Van Rooijen & de Vos, 1990). Blots were probed with PCR-amplified fragments of *mtsA* (primers LPATPF6 and LPATPR6), *mntH2* (LPMNTH2AF and LPMNTH2AR), *mntH1* (LPMNTH1F and LPMNTH1R) and *mntH3* (LPMNTH3F and LPMNTH3R). Probes were radiolabelled with [α-^{32}P]dATP by nick translation. Quantification of the transcripts in Northern blotting was performed using the Dynamics Phosphor Imaging System (Molecular Dynamics). Signal intensities were corrected for background radiation and for the total amount of RNA loaded by correlation of the signal intensity to the amount of 16S rRNA as determined by hybridization with a 700 bp PCR-amplified probe (primers 16SP1 and 16SP2). The values presented for the *mtsA* and *mntH2* mutant strains are means of two independent experiments and varied less than 12 % from the mean.

For primer extension, 20 ng oligonucleotides was annealed to 15 μg total RNA according to the method described by Kuipers *et al.* (1993). The oligonucleotides used were LPABCSEQ, LPH1SEQ and LPH2SEQ, which are complementary to the 5′ sequence of *mtsC*, *mntH1* and *mntH2*, respectively.

Real-time RT-PCR. Total RNA of cells grown at either 1·5 or 300 μM Mn^{2+} was isolated as described above and mRNA levels for *mntA*, *mntH2*, *mntH1* and *mtsA* were detected by reverse transcription (RT) followed by real-time PCR. Expression levels of the target genes were normalized using 16S rRNA levels. Prior to the RT step, RNA was treated with deoxyribonuclease I (Invitrogen Life Technologies) following the instructions of the manufacturer. RNA concentrations in the DNase-treated samples were determined using the RiboGreen RNA quantification reagent kit (Molecular Probes). Four (for samples) or 40 ng (standard curve) total RNA was reverse transcribed with Superscript II $RNaseH^-$ reverse transcriptase (Invitrogen Life Technologies) using 2 pmol either QMNTAR3, QMNTH2R, QMTSAR, QMNTH2R or Q16SREV, according to the instructions of the manufacturer. Real-time PCR products were quantified using the SYBR Green PCR mastermix (Applied Biosystems). The dynamic range and the efficiency of both target and normalizer reactions were examined by running in triplicate dilutions of the cDNA pools (0·4 pg–4 ng) using primers QMNTH2F/QMNTH2R (*mntH2*), QMNTAF3/QMNTAR3 (*mntA*), QMNTH1F/QMNTH1R (*mntH1*), QMTSAF/QMTSAR (*mtsA*) or Q16SFORW/Q16SREV (*16S*). Real-time PCR was performed on an ABI Prism 7700 sequence detector instrument (PE Applied Biosystems) in 50 μl reactions containing 25 μl SYBR Green mastermix, 2 μl forward primer (5 μM stock), 2 μl reverse primer (5 μM stock), 4 μl template (corresponding to 0·4 ng RNA per well) and 17 μl water. The following PCR conditions were used: 5 s at 50 °C and denaturation (95 °C, 10 min) followed by 40 cycles of 95 °C for 15 s followed by 54 °C for 1 min. Both target and normalizer reactions were run in triplicate and the relative error for the determination of the crossing point (CP) values was below 2 %. Relative expression levels and PCR efficiencies were calculated according to the method described by Pfaffl (2001) with the following modification: CP values of the individual samples were corrected for background values caused by small amounts of residual DNA in the RNA samples. This was done by running in triplicate real-time PCR reactions for the normalizer and for each target using RNA that was not reverse transcribed. The CP values of these samples were considered DNA-derived and the difference in CP value between the reverse transcribed and the non-transcribed sample was used for the calculation of relative expression levels of the various target genes. Statistical analysis was performed by using the REST software tool (Pfaffl *et al.*, 2002).

DNA and deduced protein analysis. Computer analysis of DNA sequences and the deduced amino acid sequences was performed using the program Clone Manager 6.0 (Scientific and Educational Software, Durham, USA). For sequence similarity searches and genome searches, the BLAST facility of the National Center for Biotechnology Information (http://www.ncbi.nlm.nih.gov) and the CLUSTALW facility of the European Bioinformatics Institute (http://www.ebi.ac.uk) were used.

RESULTS

In silico identification of putative manganese transport systems in the genome of *L. plantarum* WCFS1

The genome of *L. plantarum* WCFS1 has been sequenced (Kleerebezem *et al.*, 2003), allowing a genome-based screening to identify candidate Mn^{2+} transporters in this bacterium. Several transporter systems have been described previously for which Mn^{2+} specificity has been experimentally determined. These transporters include MntA (*L. plantarum* ATCC 14917; AAD32211), PsaA (*S. pneumoniae*; AF055088), ScaA (*S. gordonii*; P42364) and MntH (*B. subtilis*: P96593, *S. typhimurium*: Q9RPF4). Protein sequences of these transporters were used to search (TBLASTN) the *L. plantarum* WCFS1 genome and resulted in the identification of five candidate transporters. One of these was MntA (ORF *lp_1919*), the previously identified P-type ATPase for Cd^{2+} and Mn^{2+} transport in *L. plantarum* strain ATCC 14917 (Hao *et al.*, 1999b). The two *mntA* genes shared 99 % identity to each other and to a similar gene in strain NC8 (unpublished data), indicating that this gene is highly conserved within the species *L. plantarum*. One complete ABC transporter (*mtsCBA*, ORFs *lp_1095–lp_1097*) with high homology to known Mn^{2+}-specific ABC transporters of various bacteria (Table 3) and three proteins of the Nramp family (*lp_0275*, *lp_2992* and *lp_1295*) appeared to be encoded by the *L. plantarum* genome. The three Nramp-type transporters encoded by *L. plantarum* WCFS1, designated MntH1, MntH2 and MntH3, are quite homologous (pairwise identity ranging from 42 to 55 %) with MntH1 and MntH2 being the closest paralogues (55 % identity). The MntH proteins from *L. plantarum* shared a high level of identity with the MntH protein of *Lactobacillus brevis* (Hayashi *et al.*, 2001) (76, 53 and 44 % identity to MntH1, MntH2 and MntH3, respectively). In addition, the Nramp homologue encoded by the *S. mutans* genome, shared a high level of identity with the three *L. plantarum* MntH proteins (58, 54 and 45 % identity with MntH1, MntH2 and MntH3, respectively). Based on these *in silico* analyses, these five transporters were selected as targets to study their role in Mn^{2+} homeostasis in *L. plantarum*.

Table 3. Percentage identity of proteins encoded by the *mts* gene cluster in *L. plantarum* WCFS1 with ABC transporters in other bacteria

References and accession numbers: 1, Bolotin *et al.* (2001); 2, AJ276708; 3, P42364, P42361, P42360; 4, AF055088; 5, AF180520; 6, O34385, O35024, O34338; 7, AF128999; 8, AF232688.

Strain	Homology to *mts* gene product (%)			Substrate*
	MtsC	MtsB	MtsA	
L. lactis[1]	MtsB (46)	MtsC (54)	MtsA (49)	
L. casei[2]	MtsC (73)	MtsB (77)	MtsA (66)	
S. gordonii[3]	ScaC (45)	ScaB (55)	ScaA (47)	Mn^{2+}
S. pneumoniae[4]	PsaB (43)	PsaC (47)	PsaA (50)	Mn^{2+}
S. pyogenes[5]	MtsB (45)	MtsC (55)	MtsA (50)	Mn^{2+}, Fe^{2+}
B. subtilis[6]	MntB (44)	MntC (34)/MntD (35)	MntA (25)	Mn^{2+}
Sal. typhimurium[7]	SitB (33)	SitD (37)/SitC (33)	SitA (31)	Mn^{2+}
S. mutans[8]	SloA (45)	SloB (55)	SloC (50)	Mn^{2+}, Fe^{3+}

*Substrates experimentally determined.

Effect of Mn^{2+} on growth of *L. plantarum* and expression of the candidate Mn^{2+} transporters

When grown in CDM, the final culture density reached by *L. plantarum* WCFS1 was strongly affected by the Mn^{2+} concentration in the medium (Table 4). As an example, the final culture density reached in CDM containing 1·5 μM Mn^{2+} was only 34 % of that reached in CDM containing 300 μM Mn^{2+}. In addition, comparison of the intracellular Mn^{2+} concentration of strain WCFS1 grown in CDM containing 1·5 μM [0·35 ± 0·12 μg (mg protein)$^{-1}$] and 300 μM [8·4 ± 0·85 μg (mg protein)$^{-1}$] Mn^{2+} confirms the Mn^{2+} limitation for growth in CDM containing 1·5 μM Mn^{2+}. Notably, the Mn^{2+} dependency of strain WCFS1 was comparable to *L. plantarum* strain ATCC 14917 which has been reported to require 2 μM Mn^{2+} for growth (Hao *et al.*, 1999b).

To maintain Mn^{2+} homeostasis, it is likely that the expression level of dedicated Mn^{2+} transporters encoded by *L. plantarum* will be modulated in response to fluctuations of the Mn^{2+} concentration in the medium. Therefore, the expression of the transporters MntA, MtsCBA, MntH1, MntH2 and MntH3 was analysed in strain WCFS1 grown under Mn^{2+} excess and limiting conditions to substantiate the postulated role of these genes. Mn^{2+} limitation was analysed to a minimum concentration of 1·5 μM, since lower concentrations did not allow the isolation of RNA of sufficient quality due to the very limited growth of *L. plantarum* under such conditions (Table 4).

Using an *mtsA*-specific probe, a single transcript of 2·6 kb was detected in cells grown at 1·5 and 3 μM Mn^{2+}, albeit the signal intensity was significantly lower in the latter sample (Fig. 1a). This transcript size corresponds to the length required to encompass the three *mts* genes. In cells grown at Mn^{2+} concentrations above 3 μM, no *mtsA* transcript could be detected. No increase of *mtsCBA* expression was observed upon aeration as compared to anaerobic growth at 1·5 μM Mn^{2+} (results not shown). Real-time RT-PCR was used to determine the relative quantity of *mtsA*-specific mRNA in the 1·5 μM Mn^{2+} sample compared to the 300 μM Mn^{2+} sample and revealed a 29-fold increase ($P = 0·001$) in *mtsCBA* expression in the Mn^{2+}-limited cells. The transcription initiation start site of the *mtsCBA* gene cluster was determined by primer extension using RNA isolated from cells grown at 1·5 μM Mn^{2+}. Two transcription start sites, 35 and 40 nt upstream of the start codon of the *mtsC* gene were identified (Fig. 2a). These results demonstrate that *mtsC*, *B* and *A* form an operon that is activated upon Mn^{2+} starvation, which strongly supports a role of the MtsCBA system in Mn^{2+} transport.

Using *mntH1*- and *mntH2*-specific probes, single transcripts of 1·5 and 2·1 kb, respectively, were detected. The expression level of *mntH2* was strongly regulated by the Mn^{2+} concentration (Fig. 1c). A slight signal for *mntH1* was observed, although the signal intensity was lower compared

Table 4. Final optical density of *L. plantarum* WCFS1 grown in CDM at various Mn^{2+} concentrations

[Mn^{2+}] (μM)	Final OD_{600}
0	0·14 ± 0·01
0·1	0·36 ± 0·01
0·5	0·88 ± 0·01
1·5	1·43 ± 0·01
3	2·02 ± 0·12
10	2·24 ± 0·14
30	2·79 ± 0·02
100	3·81 ± 0·02
300	4·25 ± 0·09

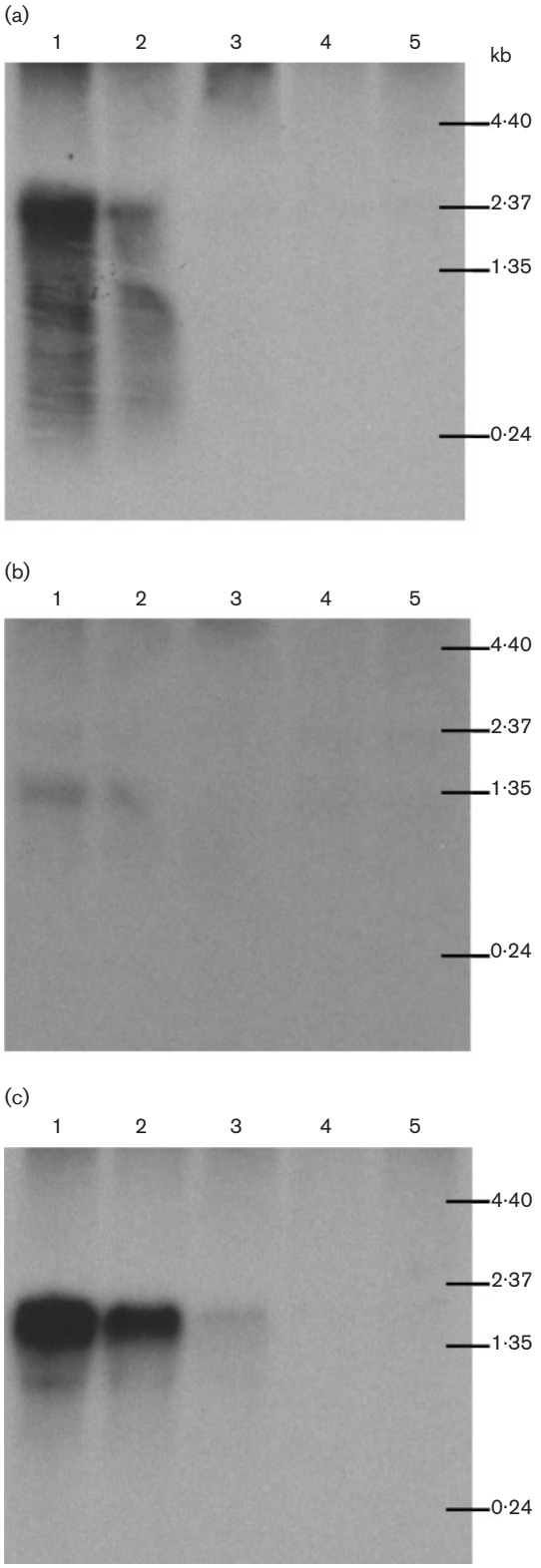

Fig. 1. Transcription analysis of *mtsCBA* (a), *mntH1* (b) and *mntH2* (c) in *L. plantarum* grown in CDM containing either 1·5, 3, 10, 100 or 300 μM of Mn^{2+} (lanes 1–5, respectively). RNA was isolated from exponentially growing cultures ($OD_{600}\approx0{\cdot}5$). Equal amounts of RNA were loaded onto a 1 % formaldehyde gel. Using an *mtsA*-specific probe, a transcript of 2·6 kb was detected. The *mntH1*-specific transcript size is about 1·5 kb and the *mntH2*-specific transcript size is about 2·1 kb.

to *mntH2* under the conditions tested (Fig. 1b). Transcripts of both genes could not be detected by Northern blotting in the range between 100 and 300 μM Mn^{2+}, while transcripts were detected at 1·5, 3 (*mntH1* and *mntH2*) and 10 μM Mn^{2+} (*mntH2*). At 1·5 μM Mn^{2+}, *mntH2* expression was increased by a factor of 294 ($P=0{\cdot}026$) and *mntH1* by 6·9 ($P=0{\cdot}001$) compared to 300 μM Mn^{2+} as determined by real-time RT-PCR. Primer extension analysis of *mntH2* revealed the presence of a single transcription initiation site located 39 nt upstream of the *mntH2* start codon (Fig. 2b). The transcript length of 2·1 kb, detected with the *mntH2*-specific probe, corresponds to the size of a bicistronic mRNA encompassing *mntH2* and a downstream-located ORF (*lp_2993*) which encodes a hypothetical protein of unknown function. Despite several attempts, no specific primer extension product for the *mntH1* gene could be identified, which might be due to the low mRNA level for this gene. In addition, the presence of a small inverted repeat in the vicinity of the *mntH1* start codon possibly prevented a successful primer extension reaction. Although the transcription initiation site for *mntH1* could not be determined, the transcript length of 1·5 kb for *mntH1* suggests that this gene is transcribed monocistronically. These results clearly show that besides MtsCBA, at least two additional candidate Mn^{2+} transport systems are induced upon Mn^{2+} starvation.

No transcripts were detected using the *mntH3*- or the *mntA*-specific probes under the conditions tested. The presence of a putative ferrochelatase-encoding gene, upstream of *mntH3*, could suggest a role for MntH3 in iron rather than Mn^{2+} transport. Expression of *mntA* under Mn^{2+} starvation has been demonstrated in *L. plantarum* strain ATCC 14917 using reverse transcriptase PCR (Hao *et al.*, 1999a), which is a more sensitive technique compared to Northern analysis. However, *mntA* expression in *L. plantarum* WCFS1 was barely detectable in our real-time RT-PCR experiments and did not appear to be significantly affected by the Mn^{2+} concentration in the medium. These data suggest that neither *mntA* nor *mntH3* plays a prominent role in maintenance of Mn^{2+} homeostasis in *L. plantarum* WCFS1 under any of the conditions tested.

Analysis of *mtsA*, *mntA* and *mntH2* mutant strains

The expression patterns of *mtsA* and *mntH2* strongly support a role of these genes in Mn^{2+} transport in *L. plantarum* WCFS1 under Mn^{2+}-limiting conditions. Therefore, these genes were selected as targets for mutation analysis in this strain. Despite the observation that strain WCFS1 did express *mntA* only at a very low level that was

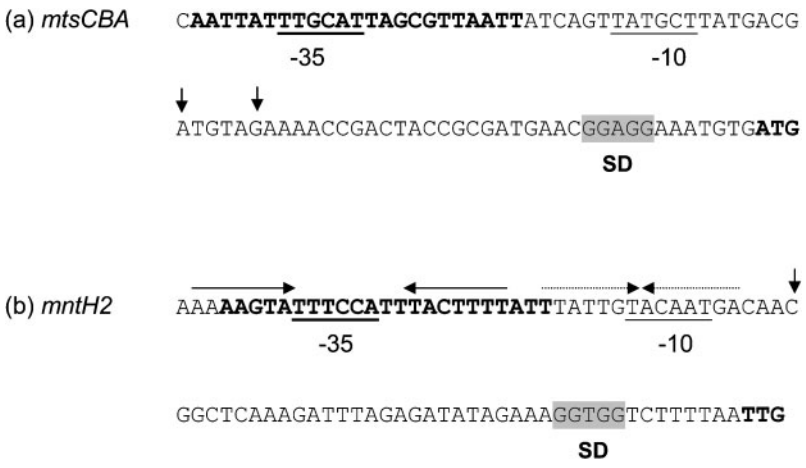

Fig. 2. Transcription initiation sites of the *mtsCBA* (a) and *mntH2* (b) genes as determined by primer extension analysis. Transcription start sites are indicated with a vertical arrow. The proposed −35 and extended −10 promoter regions are underlined. Shine–Dalgarno sequences (SD) are indicated in grey blocks. Possible *cis*-acting regulatory regions are indicated. Sequences resembling metalloregulator MntR target regions in *B. subtilis* (Que & Helmann, 2000) are indicated in bold. In addition, the *mntH2* promoter region contains two inverted repeats (indicated by arrows) that resemble the ScaR-binding site in *S. gordonii* (Jakubovics *et al.*, 2000).

not influenced by Mn^{2+} limitation, this gene was also selected as a target for mutation analysis based on the reported role of this gene in Mn^{2+} transport in strain ATCC 14917 (Hao *et al.*, 1999b).

The *mtsA* and *mntH2* genes were functionally deleted via the double cross-over strategy described in Methods, while the *mntA* gene was functionally disrupted via a single cross-over plasmid integration. Unexpectedly, the growth rates of the *mtsA*, *mntH2*, *mntA* and the *mtsA-mntH2* double mutants were not affected under Mn^{2+} limitation or excess as compared to those observed for the parent strain (Table 5). In addition, the final culture density after overnight growth of these mutants in media containing a range of Mn^{2+} concentrations was virtually identical to those observed for the wild-type strain (data not shown). Finally, the intracellular Mn^{2+} concentration in none of these mutant strains was significantly reduced compared to the parental strain under any of the conditions tested (data not shown). Notably, the *mntA* mutant strain appeared to form aggregates when grown in liquid medium under both aerobic and anaerobic conditions, independent of the Mn^{2+} concentration added to the medium. Complementation of the *mntA* mutant with a plasmid-encoded copy of *mntA* did not relieve aggregate formation (data not shown), suggesting that this phenotype results from proximal or downstream polar effects of the mutation. These growth characteristics of the *L. plantarum* WCFS1 *mntA* mutant are markedly different from those previously reported for the *mntA* mutant of strain ATCC 14917 which was unable to grow in liquid medium unless supplemented with at least 20 mM Mn^{2+} (Hao *et al.*, 1999b).

Table 5. Growth of *L. plantarum* WCFS1 wild-type and mutant strains in CDM supplemented with 1·5 or 300 μM Mn^{2+}. Aerobic incubation in shaken waterbath.

Strain	μ (h^{-1})	
	300 μM Mn^{2+}	1·5 μM Mn^{2+}
Wild-type	0·44±0·02	0·29±0·02
Δ*mtsA*	0·45±0·01	0·30±0·03
Δ*mntH2*	0·44±0·01	0·31±0·04
Δ*mtsA*Δ*mntH2*	0·43±0·01	0·31±0·03
mntA	0·48±0·02	0·33±0·04

The absence of a clear, Mn^{2+}-related phenotype in the mutant strains could possibly result from cross-regulation between transport systems. To verify this possibility, total RNA was isolated from the wild-type, the *mtsA* and *mntH2* mutants and the *mtsA-mntH2* double mutant grown in medium containing 1·5 μM Mn^{2+} for Northern analysis. Quantitative analysis of the respective transcripts on a phosphorimager revealed a slight, but significant (detected in two independent RNA isolations), increase of 50 % in *mtsCBA* transcript level in the *mntH2* mutant at 1·5 μM Mn^{2+}, compared to the parent strain grown under the same conditions. Likewise, the *mntH2* transcript level was increased by 36 % in the *mtsA* mutant strain relative to the wild-type strain under the same conditions. In contrast, the transcript levels of *mntH1* or *mntA* (the latter detected by real-time RT-PCR) were not altered in any of the mutant strains (including the *mtsA-mntH2* double mutant) when compared to the wild-type strain. These results suggest that the relative expression levels of *mtsCBA* and *mntH2* are cross-regulated and that Mn^{2+} homeostasis in *L. plantarum* is possibly tightly regulated. However, the absence of a phenotype in the *mtsA-mntH2* double mutant might suggest that additional transport systems in *L. plantarum* can accomplish Mn^{2+} uptake and have a role in Mn^{2+} homeostasis.

DISCUSSION

Intracellular accumulation of Mn^{2+} to millimolar levels by *L. plantarum* is an established and particular phenotypic characteristic of this species. The accumulated manganese acts as a protection mechanism against the damaging effects of oxygen radicals, which is proposed to occur through radical scavenging by this transition metal (Archibald &

Fridovich, 1981b). In addition, a high Mn^{2+} concentration in *L. plantarum* has been shown to play a catalytic role in the conversion of phenylalanine to benzaldehyde by this species, which is of biotechnological interest (Nierop Groot & de Bont, 1998, 1999). Finally, the γ-radiation resistance of *L. plantarum* and other lactobacilli (Hastings *et al.*, 1986) might have been facilitated by accumulated manganese as has been shown for the extremely high radiation-resistant species *Deinococcus radiodurans* (Daly *et al.*, 2004). The availability of the genome sequence of *L. plantarum* strain WCFS1 allowed the *in silico* detection of candidate manganese transporter encoding genes. Over the last few years, a considerable number of bacterial Mn^{2+} transport systems have been reported. However, besides the P-type ATPase MntA of *L. plantarum* (Hao *et al.*, 1999a) these Mn^{2+} transport systems have been studied in bacteria that only require micromolar levels of intracellular Mn^{2+}, which acts as a cofactor for SOD and several other enzymes (see Kehres & Maguire, 2003, for an overview). In this study we report the utilization of these known bacterial Mn^{2+} transport systems to query the *L. plantarum* genome sequence, leading to the identification of five candidate Mn^{2+} transport systems in this species. Besides the P-type ATPase system encoded by *mntA* that has been described in *L. plantarum* previously, three Nramp transporter homologues (*mntH1*, *mntH2* and *mntH3*) and an Mn^{2+}-specific ABC-transporter homologue (*mtsCBA*) were identified in the WCFS1 genome. Three of these five systems (*mtsCBA*, *mntH1* and *mntH2*) were found to be specifically expressed under Mn^{2+} starvation conditions, supporting their role in the maintenance of Mn^{2+} homeostasis. In contrast to previous reports, significant expression of *mntA* could not be established in *L. plantarum* WCFS1, irrespective of the Mn^{2+} concentration in the medium.

The expression of *mtsCBA* is 29-fold increased (1·5 μM compared to 300 μM Mn^{2+}) under manganese starvation in *L. plantarum*. The *L. plantarum* MtsCBA system shows a high degree of homology to systems in *Lactobacillus casei* (GenBank accession no. AJ276708) and in the *Lactococcus lactis* IL1403 genome sequence (Bolotin *et al.*, 2001), indicating that this type of cation transporter represents a common system in lactic acid bacteria. The crystal structure of the MtsA homologue in *S. pneumoniae* (PsaA) revealed that the side chains of His67, His139, Glu205 and Asp280 form the metal-binding site (Lawrence *et al.*, 1998). These four residues are conserved in the MtsA protein of *L. plantarum*. Remarkably, the N-terminal prolipoprotein signal sequence common for Gram-positive bacteria (Sutcliffe & Russel, 1995) is absent in MtsA of *L. plantarum*, but a type I signal peptidase cleavage site is predicted (Nielsen *et al.*, 1997). This suggests that in *L. plantarum*, MtsA is tethered to the cell surface via an alternative structure.

The two Nramp-type transporters that are expressed under Mn^{2+} starvation in *L. plantarum*, MntH1 and MntH2, are widespread in both Gram-positive and -negative bacteria, but are absent in *S. pneumoniae* and *S. pyogenes* genomes (Tettelin *et al.*, 2001; Ferretti *et al.*, 2001). The increased expression levels of *mntH1* (6·6-fold) and *mntH2* (294-fold) under Mn^{2+} starvation strongly suggests that these genes encode Mn^{2+} transporters. By analogy, similar genes in *B. subtilis* (Que & Helmann, 2000), *E. coli* and *Salmonella typhimurium* (Kehres *et al.*, 2000; Makui *et al.*, 2000) have been shown to be involved in Mn^{2+} transport. MntH1 and MntH2 of *L. plantarum* share a high level of identity with the HitA protein from a beer spoilage isolate of *Lactobacillus brevis*, which appeared to be expressed upon addition of bitter hop compounds (Hayashi *et al.*, 2001). Notably, one of these compounds is known to exchange extracellular protons for intracellular Mn^{2+} (Simpson, 1993), which is likely to influence intracellular Mn^{2+} levels and could support a role for HitA in Mn^{2+} transport.

Overall the expression data as well as the functional analyses of homologues of the established Mn^{2+} transport systems support a role for MntH1 and MntH2 and MtsCBA in Mn^{2+} transport. However, the *mtsA* and *mntH2* mutants and the *mtsA-mntH2* double mutant derivative of *L. plantarum* exhibited no growth defects or decreased internal Mn^{2+} levels. This is in clear contrast to similar studies in a variety of other species (Dintilhac *et al.*, 1997; Kolenbrander *et al.*, 1998; Que & Helmann, 2000; Janulczyk *et al.*, 2003; Kehres *et al.*, 2000). This may suggest that *L. plantarum* can adapt effectively to inactivation of these genes. Indeed, inactivation of *mtsA* and *mntH2* results in moderate upregulation of *mntH2* and *mtsCBA*, respectively. The increased *mtsCBA* transcript levels in the *mntH2* mutant, and vice versa, may suggest that cross-regulation occurs. Comparison of the promoter regions of *mtsC* and *mntH2* revealed the presence of possible *cis*-acting elements that could act as metalloregulator target regions based on their similarity to the MntR-binding site described for *B. subtilis* (Que & Helmann, 2000) and the ScaR-binding site described for *S. gordonii* (Jakubovics *et al.*, 2000) (Fig. 2). In the cross-regulation scenario, it remains unknown which Mn^{2+} transporter is induced in the *mntH2-mtsA* double mutant. Obvious candidates would be *mntH1* and *mntA*; however, expression of these two genes was not increased in the double mutant strain. Moreover, *mntA* disruption does not affect Mn^{2+} homeostasis in *L. plantarum* WCFS1 in contrast to the *mntA* mutant phenotype described for strain ATCC 14917 (Hao *et al.*, 1999b). Although strain-specific effects cannot be excluded, it seems likely that the ATCC 14917-derived mutant is not only affected in *mntA* but carries mutations in one or more genes involved in Mn^{2+} homeostasis.

An alternative explanation for the lack of phenotype of the mutants could be that one or more other proteins annotated as cation transporters accomplish Mn^{2+} uptake in *L. plantarum*. In *L. plantarum*, genes encoding 42 complete transport systems are present that have been annotated as cation transporters. For 13 of these transporters, the homology to transporters with experimentally verified

specificity is not sufficient to predict the substrate of these systems. Moreover, annotation of the cation specificity of transporters is a prediction and requires experimental verification to substantiate the postulated role. For example, transporters belonging to the P-type ATPase family were reported to cluster in phylogenetic trees according to their substrate specificity (Axelsen & Palmgren, 1998). However, recent studies show that two members of the calcium cluster (PMR1 from yeast and ATP2A2 from humans) actually transport Mn^{2+} into the Golgi apparatus (Maeda *et al.*, 2004; Ton *et al.*, 2002). This illustrates that prediction of the cation specificity of transporters is difficult. Interestingly, the *L. plantarum* genome is predicted to encode nine P-type ATPases, three of which resemble the recently described P-type Ca^{2+}/Mn^{2+} ATPase (PMR1) in *Schizosaccharomyces pombe* (Maeda *et al.*, 2004) (encoded by *lp_0567*, *lp_3398* and *lp_0124*). None of the bacterial homologues of this eukaryote-derived transporter has been associated with Mn^{2+} transport to date. Moreover, several bacterial homologues of this eukaryotic protein are annotated as calcium transporters. Nonetheless, a role for these transport systems in Mn^{2+} transport in *L. plantarum* appears to be a realistic option and should be targeted by future functional studies in this species.

In conclusion, although transcription analyses support the postulated role of *mntH2*, *mntH1* and *mtsA* in Mn^{2+} transport, mutation analysis has demonstrated that these genes are not essential for Mn^{2+} homeostasis in *L. plantarum* WCFS1. These findings exclude a central role for these proteins in a phenotypic characteristic that was described for *L. plantarum* several decades ago and that has been shown to fulfil highly relevant functions in this species. In addition, the results either suggest highly adaptive behaviour of *L. plantarum* in response to mutations affecting genes involved in Mn^{2+} homeostasis or could hint at the presence of alternative Mn^{2+} transporters that have not been identified in bacteria to date.

REFERENCES

Archibald, F. S. & Duong, M.-N. (1984). Manganese acquisition by *Lactobacillus plantarum*. *J Bacteriol* **158**, 1–8.

Archibald, F. S. & Fridovich, I. (1981a). Manganese, superoxide dismutase, and oxygen tolerance in some lactic acid bacteria. *J Bacteriol* **146**, 928–936.

Archibald, F. S. & Fridovich, I. (1981b). Manganese and defenses against oxygen toxicity in *Lactobacillus plantarum*. *J Bacteriol* **145**, 442–451.

Aukrust, T. & Blom, H. (1992). Transformation of *Lactobacillus* strains used in meat and vegetable fermentations. *Food Res Int* **25**, 253–261.

Axelsen, K. & Palmgren, M. G. (1998). Evolution of substrate specificity in the P-type ATPase superfamily. *J Mol Evol* **46**, 84–101.

Bartsevich, V. V. & Pakrasi, H. B. (1995). Molecular identification of an ABC transporter complex for manganese: analysis of a cyanobacterial mutant strain impaired in the photosynthetic oxygen evolution process. *EMBO J* **14**, 1845–1853.

Bearden, S. W. & Perry, R. D. (1999). The Yfe system of *Yersinia pestis* transports iron and manganese and is required for full virulence of plaque. *Mol Microbiol* **32**, 403–414.

Bolotin, A., Wincker, P., Mauger, S., Jaillon, O., Malarme, K., Weissenbach, J., Ehrlich, S. D. & Sorokin, A. (2001). The complete genome sequence of the lactic acid bacterium *Lactococcus lactis* IL1403. *Genome Res* **11**, 731–753.

Bradford, M. M. (1976). A rapid and sensitive method for the quantitation of microgram quantities of protein utilizing the principle of protein-dye binding. *Anal Biochem* **72**, 248–254.

Claverys, J.-P. (2001). A new family of high-affinity ABC manganese and zinc permeases. *Res Microbiol* **152**, 231–243.

Daly, M. J., Gaidamakova, E. K. & 11 other authors (2004). Accumulation of Mn(II) in *Deinococcus radiodurans* facilitates gamma-radiation resistance. *Science* **306**, 1025–1028.

Dintilhac, A., Alloing, G., Granadel, C. & Claverys, J.-P. (1997). Competence and virulence of *Streptococcus pneumoniae*: Adc and PsaA mutants exhibit a requirement for Zn and Mn resulting from inactivation of putative ABC metal permeases. *Mol Microbiol* **25**, 727–739.

Ferretti, J. J., McShan, W. M., Ajdic, D. & 20 other authors (2001). Complete genome sequence of an M1 strain of *Streptococcus pyogenes*. *Proc Natl Acad Sci U S A* **10**, 4658–4663.

Forbes, J. R. & Gros, P. (2001). Divalent-metal transport by NRAMP proteins at the interface of host–pathogen interactions. *Trends Microbiol* **9**, 397–403.

Hanahan, D. (1983). Studies on transformation of *Escherichia coli* with plasmids. *J Mol Biol* **166**, 557–580.

Hao, Z., Chen, S. & Wilson, D. B. (1999a). Cloning, expression, and characterization of cadmium and manganese uptake genes from *Lactobacillus plantarum*. *Appl Environ Microbiol* **65**, 4746–4752.

Hao, Z., Reiske, H. R. & Wilson, D. B. (1999b). Characterization of cadmium uptake in *Lactobacillus plantarum* and isolation of cadmium and manganese uptake mutants. *Appl Environ Microbiol* **65**, 4741–4745.

Hastings, J. W., Holzapfel, W. H. & Niemand, J. G. (1986). Radiation resistance of lactobacilli isolated from radurized meat relative to growth and environment. *Appl Environ Microbiol* **52**, 898–901.

Hayashi, N., Ito, M., Horiike, S. & Taguchi, H. (2001). Molecular cloning of a putative divalent-cation transporter gene as a new genetic marker for the identification of *Lactobacillus brevis* strains capable of growing in beer. *Appl Microbiol Biotechnol* **55**, 596–603.

Jakubovics, N. S., Smith, A. W. & Jenkinson, H. F. (2000). Expression of the virulence-related Sca (Mn^{2+}) permease in *Streptococcus gordonii* is regulated by a diphtheria toxin metallorepressor-like protein ScaR. *Mol Microbiol* **38**, 140–153.

Jakubovics, N. S., Smith, A. W. & Jenkinson, H. F. (2002). Oxidative stress tolerance is manganese (Mn^{2+}) regulated in *Streptococcus gordonii*. *Microbiology* **148**, 3255–3263.

Janulczyk, R., Ricci, S. & Björck, L. (2003). MtsABC is important for manganese and iron transport, oxidative stress resistance, and virulence of *Streptococcus pyogenes*. *Infect Immun* **71**, 2656–2664.

Kehres, D. G. & Maguire, M. E. (2003). Emerging themes in manganese transport, biochemistry and pathogenesis in bacteria. *FEMS Microbiol Rev* **27**, 263–290.

Kehres, D., Zaharik, M. L., Brett Finlay, B. & Maquire, M. E. (2000). The NRAMP proteins of *Salmonella typhimurium* and *Escherichia coli* are selective manganese transporters involved in the response to reactive oxygen. *Mol Microbiol* **36**, 1085–1100.

Kehres, D. G., Janakiraman, A., Slauch, J. M. & Maguire, M. E. (2002). SitABCD is the alkaline Mn^{2+} transporter of *Salmonella enterica* serovar Typhimurium. *J Bacteriol* **184**, 3159–3166.

Kets, E. P. W., Galinski, E. A. & de Bont, J. A. M. (1994). Carnitine: a novel compatible solute in *Lactobacillus plantarum*. *Arch Microbiol* **162**, 243–248.

Kleerebezem, M., Boekhorst, J., Van Kranenburg, R. & 17 other authors (2003). Complete genome sequence of *Lactobacillus plantarum* WCFS1. *Proc Natl Acad Sci U S A* **100**, 1990–1995.

Kolenbrander, P. E., Andersen, R. N., Baker, R. A. & Jenkinson, H. F. (1998). The adhesin-associated *sca* operon in *Streptococcus gordonii* encodes an inducible high-affinity ABC transporter for Mn^{2+} uptake. *J Bacteriol* **180**, 290–295.

Kuipers, O. P., Beerthuyzen, M. M., Siezen, R. J. & de Vos, W. M. (1993). Characterization of the nisin gene cluster *nisABTCIPR* of *Lactococcus lactis*. Requirements of expression of the *nisA* and *nisI* genes for the development of immunity. *Eur J Biochem* **216**, 281–291.

Lawrence, M. C., Pilling, P. A., Epa, V. C., Berry, A. M., Ogunniyi, A. D. & Paton, J. C. (1998). The crystal structure of pneumococcal surface antigen PsaA reveals a metal-binding site and a novel structure for a putative ABC-type binding protein. *Structure* **6**, 1553–1561.

Maeda, T., Sugiura, R., Kita, A. & 8 other authors (2004). Pmr1, a P-type ATPase, and Pdt1, an *Nramp* homologue, cooperatively regulate cell morphogenesis in fission yeast: the importance of Mn^{2+} homeostasis. *Genes Cells* **9**, 71–82.

Makui, H., Roig, E., Cole, S. T., Helmann, J. D., Gros, P. & Cellier, M. F. M. (2000). Identification of the *Escherichia coli* K-12 Nramp orthologue (MntH) as a selective divalent metal ion transporter. *Mol Microbiol* **35**, 1065–1078.

Nielsen, H., Engelbrecht, J., Brunak, S. & von Heijne, G. (1997). Identification of prokaryotic and eukaryotic signal peptides and prediction of their cleavage sites. *Prot Eng* **10**, 1–6.

Nierop Groot, M. N. & de Bont, J. A. M. (1998). Conversion of phenylalanine to benzaldehyde initiated by an aminotransferase in *Lactobacillus plantarum*. *Appl Environ Microbiol* **64**, 3009–3013.

Nierop Groot, M. N. & de Bont, J. A. M. (1999). Involvement of manganese in conversion of phenylalanine to benzaldehyde by lactic acid bacteria. *Appl Environ Microbiol* **65**, 5590–5593.

Paik, S., Brown, A., Munro, C. L., Cornelissen, C. N. & Kitten, T. (2003). The *sloABCR* operon of *Streptococcus mutans* encodes an Mn and Fe transport system required for endocarditis virulence and its Mn-dependent repressor. *J Bacteriol* **185**, 5967–5975.

Pfaffl, M. W. (2001). A new mathematical model for relative quantification in real-time RT-PCR. *Nucleic Acids Res* **29**, 2003–2007.

Pfaffl, M. W., Horgan, G. W. & Dempfle, L. (2002). Relative expression software tool (REST©) for group-wise comparison and statistical analysis of relative expression results in real-time PCR. *Nucleic Acids Res* **30**, E36.

Que, Q. & Helmann, J. D. (2000). Manganese homeostasis in *Bacillus subtilis* is regulated by MntR, a bifunctional regulator related to the diphteria toxin repressor family of proteins. *Mol Microbiol* **35**, 1454–1468.

Sambrook, J., Fritsch, E. F. & Maniatis, T. (1989). *Molecular Cloning: a Laboratory Manual*, 2nd edn. Cold Spring Harbor, New York: Cold Spring Harbor Laboratory.

Sampson, J. S., O'Connor, S. P., Stinson, A. R., Tharpe, J. A. & Russel, H. (1994). Cloning and nucleotide sequence analysis of *psaA*, the *Streptococcus pneumoniae* gene encoding a 37-kilodalton protein homologous to previously reported *Streptococcus* sp. adhesins. *Infect Immun* **62**, 319–324.

Simpson, W. J. (1993). Ionophoric action of trans-isohumulone on *Lactobacillus brevis*. *J Gen Microbiol* **139**, 1041–1045.

Sutcliffe, I. C. & Russel, R. R. B. (1995). Lipoproteins of Gram-positive bacteria. Minireview. *J Bacteriol* **177**, 1123–1128.

Tettelin, H., Nelson, K. E., Paulsen, I. T. & 36 other authors (2001). Complete genome sequence of a virulent isolate of *Streptococcus pneumoniae*. *Science* **293**, 498–506.

Ton, V.-K., Mandal, D., Vahadji, C. & Rao, R. (2002). Functional expression in yeast of the human secretory pathway Ca^{2+}, Mn^{2+}-ATPase defective in Hailey–Hailey disease. *J Biol Chem* **22**, 6422–6427.

Van Kranenburg, R., Marugg, J. D., Van Swam, I. I., Willem, N. J. & de Vos, W. M. (1997). Molecular characterization of the plasmid-encoded *eps* gene cluster essential for exopolysaccharide biosynthesis in *Lactococcus lactis*. *Mol Microbiol* **24**, 387–397.

Van Rooijen, R. J. & de Vos, W. M. (1990). Molecular cloning, transcriptional analysis, and nucleotide sequence of *lacR*, a gene encoding the repressor of the lactose phosphotransferase system of *Lactococcus lactis*. *J Biol Chem* **265**, 18499–18503.